REFERENCES

1. Liu MC, Oxnard GR, Klein EA, Swanton C, Seiden MV, on behalf of the CCGA Consortium. Sensitive and specific multi-cancer detection and localization using methylation signatures in cell-free DNA. *Ann Oncol*. 2020;31(6):745—759.
2. Taylor WC. Comment on 'Sensitive and specific multi-cancer detection and localization using methylation signatures in cell-free DNA' by M. C. Liu et al. *Ann Oncol*. 2020;31(9):1266—1267.
3. Fiala C, Diamandis EP. A multi-cancer detection test: focus on the positive predictive value. *Ann Oncol*. 2020;31(9):1267—1268.
4. Pepe MS, Etzioni R, Feng Z, et al. Phases of biomarker development for early detection of cancer. *J Natl Cancer Inst*. 2001;93(14):1054—1061.
5. Biederer J, Ohno Y, Hatabu H, et al. "Screening for lung cancer: does MRI have a role?" [European Journal of Radiology 86 (2017) 353—360]. *Eur J Radiol*. 2020;125:108896.
6. Croswell JM, Kramer BS, Kreimer AR, et al. Cumulative incidence of false-positive results in repeated, multimodal cancer screening. *Ann Fam Med*. 2009;7(3):212—222.

Unintended on-target chromosomal instability following CRISPR/Cas9 single gene targeting

Clustered regularly interspaced short palindromic repeats (CRISPR)/CRISPR-associated protein 9 (Cas9) seminal studies in mammalian cells[1—3] have resulted in gene editing being broadly adopted in basic research. However, it has become apparent that the CRISPR/Cas9 system induces unintended off- and on-target genomic alterations[4] and that there is a need for stricter clone screening methods before phenotypic characterisation is made, particularly before the technology is adopted for clinical purposes. Caution is also needed when working with cancer cell lines, as these often have underlying genomic instability and deficiencies in DNA repair or other safeguarding mechanisms which may permit large genomic deletions or rearrangements. Here, we report that CRISPR/Cas9 targeting of genes in close proximity to telomeres can result in chromosome arm truncations. We suggest assessing heterozygous single-nucleotide polymorphisms (SNPs) downstream of targeted genes to select clones without arm truncations. This screening approach could be applied alongside initial genotype assessment via sequencing at early stages of the experiment, prior to cell line expansion.

We generated CRISPR/Cas9-mediated *ZNF516* knockout (KO) cell lines to characterise the role of *ZNF516* in colorectal cancer. We used an HCT116 cell line harbouring doxycycline-inducible Cas9 (HCT116-Cas9) to restrict temporal expression of the endonuclease and minimise off-target effects. Cells were transfected with either a pool of four CRISPR RNAs (crRNAs) against *ZNF516* (sites A—D in Figure 1A) or a pool of five nontargeting crRNAs, *trans*-activating crRNA, and treated with doxycycline for 5 days to induce Cas9 expression. After single-cell sorting, clones were expanded and screened for indel mutations using Sanger sequencing. ZNF516 protein levels were assessed by western blotting and messenger RNA expression levels assessed using quantitative PCR.

To undertake biological characterisation of *ZNF516* we performed RNA-seq in two *ZNF516* KO clones (crZNF516-D7 and crZNF516-F3) and two nontargeting clones (crNT-A2 and crNT-A6), to characterise gene expression changes upon *ZNF516* KO. Unexpectedly, we observed that a large proportion of the most significantly downregulated genes were located downstream of *ZNF516* towards the telomere of 18q. This observation was suggestive of a large-scale deletion or chromosome arm truncation following Cas9-induced double-strand break (DSB) in *ZNF516*.

To investigate the potential chromosome 18q arm truncation, we assessed loss of heterozygosity (LOH) of established heterozygous HCT116 SNPs, the location of which was obtained from the Sanger COSMIC Cell Line Project's genotyping calls (https://cancer.sanger.ac.uk/cell_lines/download). We examined four heterozygous SNPs, rs1056714 located in the *ZNF516* intron between targeted exons 3 and 4, and rs17059538, rs8082885 and rs2007483 distal to *ZNF516* (Figure 1B). Sanger sequencing revealed that both *ZNF516* KO clones had LOH of all SNPs downstream of *ZNF516*. Interestingly the *ZNF516* KO clones had lost a different allele, suggesting that it was equally possible to lose either of the chromosome arms. Furthermore, rs1056714 remained heterozygous, suggesting that arm truncation was due to a Cas9-induced DSB in exon 3 of *ZNF516*.

To further confirm arm truncation, we carried out FISH on metaphase spreads from parental cell lines, *ZNF516* KO and nontargeting clones, with chromosome 18 centromeric probes and 18q subtelomeric region probe. We detected subtelomeric probe signals on both copies of chromosome 18 in all cells (50 analysed) from parental cell lines and nontargeting clones, indicating the expected presence of 18q on both chromosomes 18 in HCT116 cells. By contrast, crZNF516 clones had detectable signal on only one chromosome 18 in all cells (50 analysed; Figure 1C). Since the homologous chromosomes 18 pairs have different morphologies in the HCT116 cell line, it was possible to confirm that different chromosomes were affected in the crZNF516-D7 and crZNF516-F3 clones (Figure 1C), confirming the result from Sanger sequencing.

To identify the prevalence of this phenomenon, we utilised next-generation sequencing and sequenced DNA fragments spanning ZNF516 crRNA target sites to assess the mutation rate, and fragments spanning heterozygous SNPs to assess chromosome 18q arm truncations in parallel. Of the 155 crZNF516 clones analysed (a sum of two independent experiments), 89 (57%) had indel mutations in at least one target site. Ten (6%) crZNF516 clones had LOH of all three SNPs below *ZNF516*, of which five also had LOH of the intronic SNP, suggesting arm truncation could occur due to DSB either in exon 3 or exon 4 (Table 1). Of the 107 crNT clones analysed (a sum of two independent experiments), none had indel mutations and one (1%) had LOH of all four SNPs analysed, suggesting that active Cas9 and/or transfection with nontargeting crRNAs could also induce large deletions.

In parallel, we transfected HCT116-Cas9 cells with an individual crRNA ('A', 'B', 'C' or 'D'; target sites shown in Figure 1A) to investigate whether this would have the same effect as the pool of four crRNAs. Depending on the crRNA used,

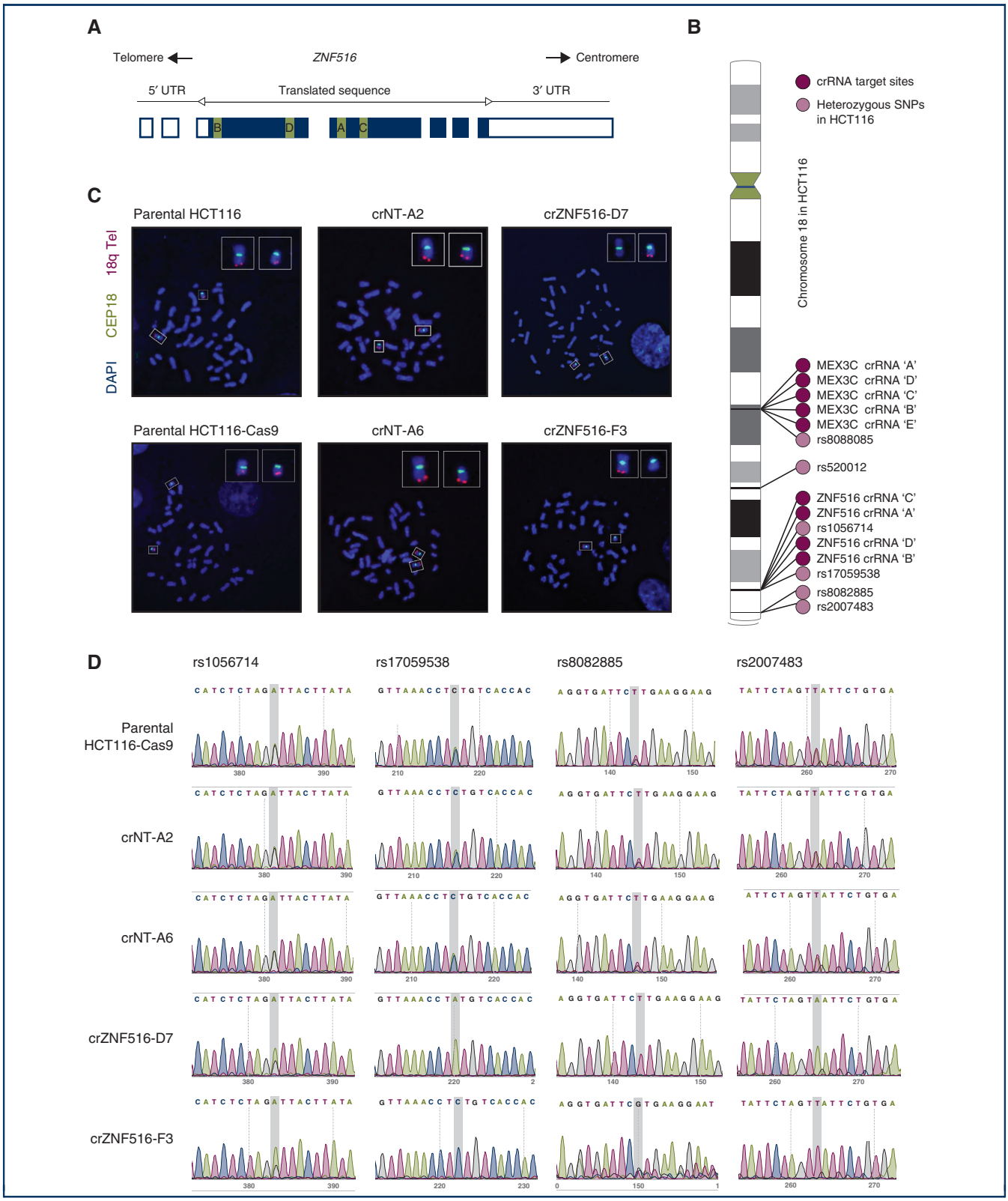

Figure 1. Detection of chromosome 18q arm truncation following CRISPR/Cas9 targeting of *ZNF516*.
(A) Schematic of 7 exons of *ZNF516* on the reverse strand, with coding sequence shown as filled rectangles, and untranslated regions as empty rectangles. crRNA target sites are indicated in green in exon 3 and 4. (B) Schematic of heterozygous SNP location on chromosome 18 in HCT116. Schematic was made with Phenogram created by Ritchie Lab (2012). (C) FISH on metaphase spreads stained with DAPI (blue) and hybridised to a chromosome 18 centromere probe (green) and 18q subtelomeric region probe (red). (D) Sanger sequencing traces of four heterozygous SNPs in HCT116. rs1056714 is located in the *ZNF516* intron between crRNA-targeted exons 3 and 4. The rest of the SNPs are located distal to *ZNF516* and towards the telomere. crRNA, CRISPR (clustered regularly interspaced short palindromic repeats) RNA; DAPI, 4′,6-diamidino-2-phenylindole; SNP, single-nucleotide polymorphism; UTR, untranslated region.

Table 1. Prevalence of LOH of heterozygous SNPs following CRISPR/Cas9 targeting.

Cell line	Targeted gene	crRNA	Clones analysed	Clones with indels	Number of clones with indels at					Any SNP LOH	All ds[a] SNP LOH
					Target site 'A'	Target site 'B'	Target site 'C'	Target site 'D'	Target site 'E'		
HCT116	Nontargeting	Pool of 5 (Exp 1)	66	0	0	0	0	0	—	2 (3%)	0
HCT116	*ZNF516*	Pool of 4 (Exp 1)	96	65 (68%)	0	57 (59%)	21 (22%)	22 (23%)	—	35 (36%)	6 (6%)
HCT116	Nontargeting	Pool of 5 (Exp 2)	41	0	0	0	0	0	—	1 (2%)	1 (2%)
HCT116	*ZNF516*	Pool of 4 (Exp 2)	59	24 (40%)	20 (33%)	6 (10%)	1 (2%)	2 (3%)	—	6 (10%)	4 (7%)
HCT116	*ZNF516*	crRNA 'A'	58	33 (57%)	33 (57%)	—	—	—	—	5 (9%)	4 (7%)
HCT116	*ZNF516*	crRNA 'B'	48	17 (35%)	—	17 (35%)	—	—	—	2 (4%)	1 (2%)
HCT116	*ZNF516*	crRNA 'C'	47	4 (9%)	—	—	4 (9%)	—	—	3 (6%)	1 (2%)
HCT116	*ZNF516*	crRNA 'D'	53	13 (25%)	—	—	—	13 (25%)	—	3 (6%)	2 (4%)
HCT116	Nontargeting	Pool of 5	58	0	0	0	0	0	0	1 (2%)	0
HCT116	*MEX3C*	Pool of 5	52	15 (29%)	0	5 (10%)	2 (4%)	10 (19%)	1 (2%)	0	0

crRNA, CRISPR (clustered regularly interspaced short palindromic repeats) RNA; LOH, loss of heterozygosity; SNP, single-nucleotide polymorphism.
[a] ds, downstream from the targeted gene towards the telomere.

mutation rates varied from 9% for crRNA 'C' to 57% for crRNA 'A' (Table 1). The proportion of samples affected by LOH of all heterozygous SNPs downstream of *ZNF516* varied between 2% for crRNA 'C' and 7% for crRNA 'A', indicating that perhaps the efficiency of a particular crRNA to induce mutation could correlate with its efficiency of chromosome arm truncation. Results for all crRNA target sites are summarised in Table 1.

Finally, we targeted *MEX3C* located further away from the telomere than *ZNF516*, with a pool of five crRNAs (Figure 1B) to investigate whether proximity to the telomere influences arm truncation prevalence. Of the 52 crMEX3C clones analysed, 15 (29%) had indel mutations and none had LOH of the two SNPs analysed below *MEX3C* (rs8088085 and rs520012; Figure 1B; Table 1). Of the 58 crNT clones analysed, none had indel mutations and one (2%) had LOH of rs8088085, again suggesting that active Cas9 and/or transfection with nontargeting crRNAs could also induce large deletions.

In this study we demonstrate that CRISPR/Cas9 targeting can induce inadvertent arm truncation. While the existence of a low-background LOH of 18q in parental HCT116-Cas9 cells is a possibility even without CRISPR/Cas9 intervention, it seems that targeting genes with close proximity to telomeres could elevate the extent of chromosomal arm deletions compared with a commonly used nontargeting control.

Two studies[5,6] previously reported incidental chromosome arm truncation following CRISPR/Cas9 targeting telomere-proximal genes: *POLE*[5] located 11 kb and *UROS*[6] located 6 million bp away from chromosome arm end. *ZNF516* is located 6 million bp from the telomere, whereas *MEX3C*, targeting which did not induce arm truncation, is located 31 million bp away from the arm end. This could suggest that targeting genes close to telomeres could result in arm truncations. Reports by Rayner et al.[5] and Cullot et al.[6] suggested detection of arm truncation with FISH analysis for targeted genes; however, this can only be achieved after cell colony expansion and involves several experimental steps. We suggest assessing heterozygous SNPs downstream of targeted genes in addition to initial mutation analysis and genotype confirmation via sequencing. This methodology could preselect clones with correct genotype and without arm truncations before further cell line expansion for future downstream characterisation.

J. Przewrocka[1,2], A. Rowan[1], R. Rosenthal[1], N. Kanu[2,†] & C. Swanton[1,2,†]*
[1]*The Francis Crick Institute, London;*
[2]*University College London, London, UK*
(*E-mail: charles.swanton@crick.ac.uk).
[†]Joint corresponding authors.

Available online 15 May 2020

https://doi.org/10.1016/j.annonc.2020.04.480

ACKNOWLEDGEMENTS

We thank Dr Ming Jiang and Dr Michael Howell for provision of the HCT116-Cas9 cell line; Dr Tom Watkins for provision of resources for heterozygous SNPs selection; Jeff Li and Haoran Zhai for contribution to MiSeq library preparation; Dr Maria Greco and Laura Cubitt for processing samples before sequencing; Dr Panos Zalmas, Dr Eva Grönroos, Dr Su Kit Chew and Dr Harshil Patel for their continued advice.

CONFLICT OF INTEREST

J.P, N.K and A.R. declare no conflict of interests. R.R. has stock options in and has consulted for Achilles Therapeutics. C.S. acknowledges grant support from AstraZeneca, BMS, Roche-Ventana, Boehringer-Ingelheim and Ono Pharmaceutical and Pfizer. C.S. has consulted for Pfizer, Novartis, GlaxoSmithKline, MSD, BMS, Celgene, AstraZeneca, Illumina, Genentech, Roche-Ventana, GRAIL, Medicxi, and the Sarah Cannon Research Institute. C.S. has stock option in Apogen Biotechnologies, Epic Bioscience, GRAIL, and has stock options and is co-founder of Achilles Therapeutics.

FUNDING ACKNOWLEDGMENT AND DISCLOSURE

This work was supported by the Francis Crick Institute that receives its core funding from Cancer Research UK (FC001169), the UK Medical Research Council (FC001169), and the Wellcome Trust (FC001169).

J.P. PhD studentship was funded by the European Research Council (ERC) under the European Union's Seventh Framework Programme (FP7/2007-2013) Consolidator Grant (FP7-THESEUS-617844).

A.R. receives funding from the Francis Crick Institute that receives its core funding from Cancer Research UK (FC001169), the UK Medical Research Council (FC001169), and the Wellcome Trust (FC001169).

R.R. receives funding from the Royal Society Enhancement Award.

N.K. receives funding from Cancer Research UK.

C.S. is Royal Society Napier Research Professor. **C.S.** is funded by Cancer Research UK (TRACERx, PEACE and CRUK Cancer Immunotherapy Catalyst Network), Cancer Research UK Lung Cancer Centre of Excellence, the Rosetrees Trust, Butterfield and Stoneygate Trusts, Novo-Nordisk Foundation (ID16584), the NIHR BRC at University College London Hospitals, and the CRUK-UCL Centre, Experimental Cancer Medicine Centre, and the Breast Cancer Research Foundation (BCRF). This research is supported by a Stand Up To Cancer-LUNGevity-American Lung Association Lung Cancer Interception Dream Team Translational Research Grant (Grant Number: SU2C-AACR-DT23-17). Stand Up To Cancer is a program of the Entertainment Industry Foundation. Research grants are administered by the American Association for Cancer Research, the Scientific Partner of SU2C. **C.S.** receives funding from the European Research Council (ERC) under the European Union's Seventh Framework Programme (FP7/2007-2013) Consolidator Grant (FP7-THESEUS-617844), European Commission ITN (FP7-PloidyNet 607722), an ERC Advanced Grant (PROTEUS) from the European Research Council under the European Union's Horizon 2020 research and innovation programme (grant agreement No. 835297), and Chromavision from the European Union's Horizon 2020 research and innovation programme (grant agreement 665233).

REFERENCES

1. Jinek M, East A, Cheng A, Lin S, Ma E, Doudna J. RNA-programmed genome editing in human cells. *eLife*. 2013;2013:1—9.
2. Cong L, Ran FA, Cox D, et al. Multiplex genome engineering using CRISPR/Cas systems. *Science*. 2013;339:819—823.
3. Mali P, Yang L, Esvelt KM, et al. RNA-guided human genome engineering via Cas9. *Science*. 2013;339:823—826.
4. Kosicki M, Tomberg K, Bradley A. Repair of double-strand breaks induced by CRISPR-Cas9 leads to large deletions and complex rearrangements. *Nat Biotechnol*. 2018;36:765—771.
5. Rayner E, Durin MA, Thomas R, et al. CRISPR-Cas9 causes chromosomal instability and rearrangements in cancer cell lines, detectable by cytogenetic methods. *CRISPR J*. 2019;2:406—416.
6. Cullot G, Boutin J, Toutain J, et al. CRISPR-Cas9 genome editing induces megabase-scale chromosomal truncations. *Nat Commun*. 2019;10:1—14.

Tocilizumab for refractory severe immune checkpoint inhibitor-associated myocarditis

Despite the availability of multiple immunosuppression methods, refractory immune checkpoint inhibitor-associated myocarditis remains a life-threatening toxicity associated with a high mortality of ∼40% as well as severe infectious complications.[1] Here we report a case of a 57-year-old male receiving third-line treatment with a combination of checkpoint inhibitors (nivolumab and ipilimumab) for metastatic lung small-cell neuroendocrine carcinoma, stage IIIB. Before receiving the third treatment cycle, he presented a muscular weakness of the lower limbs with dyspnea of sudden onset associated with an oppressive retrosternal chest pain without syncope and a ptosis of the right eye with diplopia. He subsequently developed severe arrhythmias and third-grade atrioventricular block. Elevated concentrations of high-sensitivity troponins I and T, creatine kinase (CK), ferritin (Figure 1) and positron emission tomography/computed tomography with ^{68}Ga-DOTATOC (gallium-68 DOTA-DPhe1, Tyr3-octreotate) confirmed the diagnosis of generalized myositis complicated by myocarditis and ocular myositis (see supplementary Figure S1, available at *Annals of Oncology* online). The left ventricular ejection fraction was preserved and coronary angiography showed normal arteries. A very broad infectious and myasthenia panel was negative. A myocarditis—myositis overlap syndrome was diagnosed and a pacemaker was placed. He received methylprednisolone sodium succinate pulse therapy at a dose of 1 g/day for 1 day followed by a dose of 200 mg/day for 5 days. Despite the repeated administrations of high intravenous methylprednisolone over a 1-week period, the patient's troponin I and T, CK and ferritin levels increased quickly (from 1291 to 18522 μg/l; Figure 1). The HScore was 211 points with a 93%—96% probability for associated reactive hemophagocytic syndrome. Intravenous tocilizumab (TCZ; at a dose of 8 mg/kg body weight weekly for two doses) was administered. The troponin T/I, CK and ferritin levels as well as inflammatory parameters rapidly decreased (Figure 1). The ejection fraction remained normal, and symptoms of myocarditis (arrhythmias) and myositis (muscular weakness and pain) progressively disappeared. Corticosteroids were progressively tapered and the patient did not experience any recurrence of cardiac or myositis adverse events. The immunotherapy was discontinued.

Severe and refractory immune checkpoint inhibitor-related myocarditis represents an important clinical challenge due to its high mortality, despite the use of immunosuppression escalation and the availability of multiple immunosuppressant (IS) drugs such as infliximab, rituximab, tacrolimus, antithymocyte globulin, mycophenolate mofetil or tacrolimus. The successful use of abatacept[2] and alemtuzumab,[3] two selective IS drugs, has been recently reported for this condition.

Interleukin (IL)-6 is a critical driver of acute and chronic inflammation. During inflammation, IL-6 signaling drives